Generalization of Nosé and Nosé-Hoover isothermal dynamics

A. C. Brańka and K. W. Wojciechowski
Institute of Molecular Physics, Polish Academy of Sciences, Smoluchowskiego 17/19, 60-179 Poznań, Poland
(Received 1 March 2000; revised manuscript received 28 April 2000)

The infinitely many possible isothermal dynamics based on Nosé and Nosé-Hoover methods are investigated. Their properties and criteria for selecting different isothermal dynamics determined by various scaling functions of the thermostat s variable involved in the generalized Nosé Hamiltonian [J. Jellinek and R. S. Berry, Phys. Rev. A **38**, 3069 (1988)] are tested with molecular dynamics simulations, and examined analytically. It is shown that time scaling is related to the scaling of the momenta. It is demonstrated that, for practical realizations, the entire generalization of the Nosé-Hoover method reduces to only two momentum scaling functions h and u, with a function v defining the ''potential energy'' of the thermostat. The most general form of the generalized Nosé-Hoover (GNH) equations of motion is established. It enables correct calculations of both static and dynamic equilibrium quantities. GNH equations with $h=s^{\alpha}$, $u=s^{\vartheta}$, and $v\sim lns$ are studied in detail. With such a choice of the functions the extended Nosé-Hoover (ENH) equations are expected to produce more chaotic phase-space dynamics than the NH equations. This is illustrated by thermalization of a one dimensional harmonic oscillator. For a system away from equilibrium the ENH thermostat is not able to provide dynamics consistent with the target temperature, and, thus, the GNH approach reduces to the original Nosé-Hoover thermostat. A simple modification of the ENH equations is proposed which makes the ENH thermostat also applicable to nonequilibrium states.

PACS number(s): 05.10.−a, 05.20.Jj, 02.70.Ns, 05.70.Ln

I. INTRODUCTION

During the last 25 years molecular dynamics (MD) simulations at other than ordinary isoenegetic conditions have become possible [1–4]. Many methods for performing calculations at different thermodynamic conditions (such as constant temperature or constant pressure) have been developed, extending molecular dynamics simulations to various ensembles (for a review, see, for instance, Refs. [5,6]). Among these methods calculations at constant temperature are particularly useful, and so have attracted considerable attention. Continuous interest in this subject is driven by applications in the area of nonequilibrium simulations. In these, heat production in the system requires a thermostatting mechanism to achieve steady-state conditions [7,8].

Among the many approaches to achieving constant temperature conditions, one of the most important was invented by Nosé [9,10]. It is based on extending the space of the coordinates and momenta of the real particles by adding an extra ''virtual'' variable along with its conjugate momentum. A specific Hamiltonian is proposed in which the extra degrees of freedom act as a heat bath for the real particles, which guarantees that the equations of motion of the resulting ''extended'' system generate time averages that are equivalent to the canonical ensemble averages.

Hoover [11] reformulated and simplified the extended system method, making it more useful for implementation in MD calculations. In both approaches a major advance was achieved by showing that the canonical distribution of particle positions and momenta can be generated with smooth, deterministic, and time-reversible trajectories. At present the Nosé-Hoover approach is a primary tool for performing constant temperature calculations both at and away from equilibrium.

Many modifications and generalizations based on the Nosé's Hamiltonian and Hoover's scheme were proposed in the literature [12–17]. The many alternative constant temperature dynamics techniques proposed create the impression that we have at hand a large number of powerful tools to investigate dynamical models, and that with these tools we have considerably extended our capability to simulate not only static but also transport and time-dependent properties of different dynamical systems.

Among the various proposals, an approach by Jellinek and Berry [12] appears to be the most comprehensive. Jellinek and Berry proposed a generalization of the Nosé Hamiltonian involving multiplicative scaling of coordinates, momenta, and time. They concluded that there exist infinitely many *different* Hamiltonians (nonequivalent dynamics) which possess *all* the properties of Nosé's Hamiltonian dynamics. These proposed generalized dynamics have not been exploited in practical applications, and the criteria for selecting for a given type of dynamics have not been established. The present work attempts to fill this gap.

In this work we have searched for the possible advantages and disadvantages of such generalized dynamics. We show that the number of generalized Hamiltonians which possess the properties of the Nosé Hamiltonian is in fact quite small. Thus our freedom to select a method for generating isothermal dynamics is also quite limited.

In Sec. II the Nosé and Nosé-Hoover approaches are briefly introduced. Their generalizations are presented in Sec. III. Implications of the position and momentum scaling are investigated in Secs. IV and V, respectively. Additional scaling of the virtual momenta is considered in Sec. VI. Equilibrium and nonequilibrium properties of the generalized Nosé-Hoover scheme are studied and discussed in Secs. VII and VIII. Conclusions are drawn in Sec. IX.

II. NOSÉ AND NOSÉ-HOOVER DYNAMICS

In the Nosé approach [9,10] a physical system of N particles with momenta $\mathbf{p}'=(\mathbf{p}_1',\mathbf{p}_2',\ldots,\mathbf{p}_N')$ and coordinates

$\mathbf{q}'=(\mathbf{q}_1',\mathbf{q}_2',\ldots,\mathbf{q}_N')$ in a fixed volume V', and potential energy $U(\mathbf{q}')$, is considered. An additional degree of freedom s' is introduced and two phase spaces, or systems, are defined: the extended virtual system (primed variables) $\Gamma' \equiv(\mathbf{q}',\mathbf{p}',s',P_s')$, and the extended physical system (unprimed variables) $\Gamma\equiv(\mathbf{q},\mathbf{p},s,P_s)$, where P_s' is the conjugate momentum of s'. (Note that previously the virtual system has most commonly been characterized by unprimed variables.) The physical system $(\mathbf{q},\mathbf{p})$ is a subsystem of the extended physical system. The relationship between the two phase spaces (unprimed and primed variables) is defined as

$$\mathbf{q}=\mathbf{q}', \quad \mathbf{p}=\mathbf{p}'/s', \quad s=s', \quad P_s=P_s'/s', \quad dt=dt'/s', \tag{1}$$

and the following Hamiltonian is postulated for the extended virtual system:

$$H_{\mathcal{N}}'=\sum_{i=1}^{N}\frac{\mathbf{p}_i'^2}{2ms'^2}+U(\mathbf{q}')+\frac{P_s'^2}{2Q}+gkTlns'. \tag{2}$$

The parameter g is essentially equal to the number of degrees of freedom of the physical system, m is the mass of the particle, Q is a parameter which acts as an effective ''mass'' for the motion of s, k is Boltzmann's constant, and T is the temperature. In the extended virtual system the total energy is conserved and we have a situation resembling traditional (E,V,N) microcanonical MD simulations. If we assume the quasiergodic hypothesis, then time averages along the trajectory determined by the equations of motion are equal to ensemble averages in the microcanonical ensemble, with the partition function

$$Z_\mu=\frac{1}{N!}\int dP_s'\int ds'\int d\mathbf{p}'\int d\mathbf{q}'\,\delta(H_{\mathcal{N}}'-E). \tag{3}$$

The essence of Nosé's approach is a simple relation between the microcanonical partition function of the extended virtual system and the canonical partition function of the physical system, Z_c,

$$Z_\mu=\frac{C}{N!}\int d\mathbf{p}\int d\mathbf{q}\exp[-H(\mathbf{p},\mathbf{q})/kT]\equiv CZ_c, \tag{4}$$

where $H=\Sigma\mathbf{p}_i^2/2m+U(\mathbf{q})$ is a Hamiltonian for the physical system, and $C(T,Q,E,N)$ is a constant. This relation forces the time averages of any quantity which is a function of $\mathbf{p}'/s'$ and $\mathbf{q}'$ along the trajectory determined by the equations of motion to be exactly those of the canonical ensemble:

$$\lim_{t'\to\infty}\frac{1}{t'}\int_0^{t'}A(\mathbf{p}'/s',\mathbf{q}')d\tau'=\langle A(\mathbf{p}'/s',\mathbf{q}')\rangle_\mu=\langle A(\mathbf{p},\mathbf{q})\rangle_c. \tag{5}$$

$\langle\cdots\rangle_\mu$ and $\langle\cdots\rangle_c$ denote the microcanonical ensemble average in the extended virtual system and the canonical ensemble average in the physical system, respectively. The Hamiltonian dynamics in the extended virtual space generates fluctuations of the kinetic and potential energies in the physical system, in accordance with canonical distributions of the $(\mathbf{p},\mathbf{q})$ -variables at the fixed temperature T.

In practical realizations, Nosé's scheme in the phase space of virtual variables is so cumbersome (mainly due to a nonphysical time scaling involved in it) that calculations of time-correlation functions with this scheme are hardly feasible. This difficulty is avoided by transforming Hamiltonian equations of motion in Γ' space into non-Hamiltonian equations of motion in Γ space, employing the scaling relation [Eq. (1)] between both spaces [10,11]. The resulting equations of motion in the extended physical space allow one to propagate directly the physical coordinates and momenta. Hoover pointed out that for the thermostatting mechanism only the product of s and P_s is significant. Defining $\zeta=sP_s/Q$, he transformed the equations of motion into a closed set of equations in the $(\mathbf{p},\mathbf{q},\zeta)$ space,

$$\frac{d\mathbf{q}_i}{dt}=\frac{\mathbf{p}_i}{m}, \tag{6}$$

$$\frac{d\mathbf{p}_i}{dt}=-\frac{\partial U}{\partial\mathbf{q}_i}-\zeta\mathbf{p}_i, \tag{7}$$

$$\frac{d\zeta}{dt}=\frac{1}{Q}\left(\sum_i\frac{\mathbf{p}_i^2}{m}-gkT\right), \tag{8}$$

with the subsidiary equation for s,

$$\frac{ds}{dt}=s\zeta, \tag{9}$$

which is not needed to compute the trajectories of the N interacting particles. A conserved quantity for this system is

$$\Upsilon=\sum_i\frac{\mathbf{p}_i^2}{2m}+U(\mathbf{q})+\frac{1}{2}Q\zeta^2+gkTlns, \tag{10}$$

which is not a Hamiltonian. The set of the equations of motion (6)–(9) defines ''Nosé-Hoover'' (NH) dynamics. As was shown by Hoover [11], these equations generate the stationary phase-space density

$$\mathcal{F}_c\propto\exp\left(-\frac{1}{kT}\left(\sum_i\frac{\mathbf{p}_i^2}{2m}+U(\mathbf{q})+\frac{1}{2}Q\zeta^2\right)\right), \tag{11}$$

which satisfies the continuity equation for the probability density function $\mathcal{F}$. Conservation of canonical distribution (11) is a necessary, but not sufficient, condition for establishing the equivalence of time averages generated by the non-Hamiltonian dynamics to corresponding canonical ensemble averages [8]. In the NH approach such an equivalence can be established via the extended phase space of virtual variables in three separate conceptual steps [12,18,19]. The first step establishes an *ensemble-ensemble* relation [i.e., the second equality in relation (5)], by exploiting relation (4) between canonical and microcanonical partition functions. The second step establishes an *ensemble-dynamics* relation in the phase space of the virtual variables based on the von Neumann–Birkhoff theorem [20] which justifies the use of the ensemble average instead of the time average. In the third step the *dynamics-dynamics* relation between the primed and unprimed dynamics (or equations of motion) is achieved us-

ing the scaling relation (1) and demonstrates that the time propagators of the two dynamics are equivalent [21,18].

It is worth noting that transformation (1), consisting of the virtual momentum and nonphysical time scaling, can be performed not in one but in two stages. If in the first stage only time scaling is performed, the resulting equations become real or physical time equations of motion of the virtual variables $(\mathbf{q}',\mathbf{p}',P_s',s')$. Then it can be readily demonstrated that such equations of motion can be directly derived from a particular Hamiltonian which is the constrained Nosé Hamiltonian, $H_{\mathcal{N}}'=0$, multiplied by the s' variable. This particular Hamiltonian, $H_{\mathcal{D}}'=s'H_{\mathcal{N}}'$, was discovered by Dettmann [8] (see also [22]), and avoids the time transformation involved in a derivation of the NH equations from Nosé's Hamiltonian. The Hamiltonian of Dettmann can be considered as an intermediate step in the dynamics-dynamics relation between the Nosé and NH dynamics, or as an alternative and simpler means of deriving NH dynamics. The Nosé-Hoover scheme solved the problem of performing MD simulations at constant temperature, and has become a standard simulation method.

III. GENERALIZATIONS OF NOSÉ'S ISOTHERMAL DYNAMICS

Jellinek and Berry [12] demonstrated that Nosé's dynamics is not unique. In fact, there exist many other different dynamics which are defined by the *generalized* Nosé Hamiltonian,

$$H_{G\mathcal{N}}'=\sum_i \frac{\mathbf{p}_i'^2}{2mh_i^2(s')}+U(f(s')\mathbf{q}')+\frac{P_s'^2}{2u(s')Q}+kTv(s'), \tag{12}$$

where $h_i(s')$, $f_i(s')$, $u(s')$, and $v(s')$ are real nonvanishing differentiable functions of s'. For $h(s')=s'$, $f(s')=1$, $u(s')=1$, and $v(s')=g\ln s'$, the original Nosé Hamiltonian is recovered. The generalized Hamiltonian equations of motion are

$$\frac{d\mathbf{q}_i'}{dt'}=\frac{\mathbf{p}_i'}{mh_i^2}, \tag{13}$$

$$\frac{d\mathbf{p}_i'}{dt'}=-\frac{\partial U}{\partial \mathbf{q}_i'}, \tag{14}$$

$$\frac{ds'}{dt'}=\frac{P_s'}{u^2Q}, \tag{15}$$

$$\frac{dP_s'}{dt'}=\sum_i \frac{\mathbf{p}_i'^2}{mh^3}\frac{dh_i}{ds'}-\frac{\partial U}{\partial s'}+\frac{P_s'^2}{u^3Q}\frac{du}{ds'}-kT\frac{dv}{ds'}. \tag{16}$$

The generalized Hamiltonian makes it possible to search for equations of motions able to mimic, both adequately and more efficiently, not only the equilibrium but also the time-dependent properties of a given physical system. To our knowledge this possibility has not been explored in the literature in any systematic way. We are aware of only a few applications of particular generalized isothermal dynamics. Winkler [15], for example, argued that the cases $h(s')=s'^2$, $f(s')=1$, $u(s')=1$, and $v(s')=g\ln s'$ give better mixing of phase-space trajectories in systems with a few degrees of freedom.

The relation between virtual and physical spaces (or between unprimed and primed variables) is defined as

$$\mathbf{q}_i=\mathbf{q}_i' f_i, \quad \mathbf{p}_i=\mathbf{p}_i'/h_i, \quad s=s', \quad P_s=P_s'/u, \quad dt=dt'/w, \tag{17}$$

where w is a real nonvanishing differentiable function of s'. The above scaling relations lead to the following equations of motion in the extended physical space, which we call generalized Nosé-Hoover (GNH) dynamics:

$$\frac{d\mathbf{q}_i}{dt}=\frac{f_i w}{h_i}\frac{\mathbf{p}_i}{m}+\frac{1}{f_i}\frac{df_i}{ds}\frac{w}{uQ}P_s\mathbf{q}_i, \tag{18}$$

$$\frac{d\mathbf{p}_i}{dt}=-\frac{f_i w}{h_i}\frac{\partial U}{\partial \mathbf{q}_i}-\frac{1}{h_i}\frac{dh_i}{ds}\frac{w}{uQ}P_s\mathbf{p}_i, \tag{19}$$

$$\frac{ds}{dt}=\frac{w}{uQ}P_s, \tag{20}$$

$$\frac{dP_s}{dt}=\frac{w}{u}\left(\sum_i \frac{\mathbf{p}_i^2}{m}\frac{1}{h_i}\frac{dh_i}{ds}-\sum_i \mathbf{q}_i\frac{\partial U}{\partial \mathbf{q}_i}\frac{1}{f_i}\frac{df_i}{ds}-kT\frac{dv}{ds}\right). \tag{21}$$

The equivalence between the above GNH dynamics and canonical ensemble averages of physical quantities can be established in the same way as for the NH dynamics—by using the ensemble-ensemble, ensemble-dynamics, and dynamics-dynamics relations [12,18]. In accordance with these three steps the GNH equations of motion (18)–(21) generate the canonical distribution for the physical phase-space variables or time averages calculated along trajectories generated by the GNH equations are equivalent to the canonical ensemble averages.

It is worth mentioning that, parallel to NH dynamics, an ''intermediate'' Hamiltonian can be found which avoids the unphysical time scaling in deriving the GNH dynamics from the generalized Nosé Hamiltonian. This Hamiltonian has the form $H_{G\mathcal{D}}'=wH_{G\mathcal{N}}'$, and requires the additional condition $H_{G\mathcal{N}}'=0$. The implications of the various scaling functions involved in the GNH dynamics are the subject of the next sections.

IV. SCALING OF PARTICLE POSITIONS

Let us first assume that for each particle i, $f_i=f$ and $h_i=h$. Furthermore, in order to concentrate on the q-scaling problem and to make our considerations more specific, let us further assume $h=s^2$ and $f=s$ and, similarly to the NH dynamics, $u\equiv 1$, $w=s$, and $v=g\ln s$. For such a form of the scaling functions the GNH equations read,

$$\frac{d\mathbf{q}_i}{dt}=\frac{\mathbf{p}_i}{m}+\zeta\mathbf{q}_i, \tag{22}$$

$$\frac{d\mathbf{p}_i}{dt}=-\frac{\partial U}{\partial \mathbf{q}_i}-2\zeta\mathbf{p}_i, \tag{23}$$

$$\frac{d\zeta}{dt}=\frac{1}{Q}\left(2\sum_i \frac{\mathbf{p}_i^2}{m}-\sum_i \mathbf{q}_i\frac{\partial U}{\partial \mathbf{q}_i}-gkT\right), \tag{24}$$

$$\frac{ds}{dt}=s\zeta, \tag{25}$$

where P_s/Q has been replaced by ζ. The equation for the variable s is, just as in the case of the NH dynamics, the subsidiary equation. The conserved quantity here has exactly the same form as that in Eq. (10). (Note that a similar situation can be achieved with *any* $h=sf$, and $f=s^l$, where l is a real number.) It is also easy to check that the canonical phase-space density given in Eq. (11) is a stationary solution of the continuity equation for the probability density in the phase space of the above GNH equations. Thus the necessary condition to simulate canonical ensemble averages is fulfilled.

In order to study properties of the GNH equations, we first consider a system of particles in an external potential $\varphi(x,y,z)=b(x^\kappa+y^\kappa+z^\kappa)/\kappa$ which localizes the particles in the space. [In such a system there are no complications from the periodic boundaries due to the position dependent forces present in Eqs. (22) and (23)]. This external potential mimics a cubic container confining the system of interacting particles. The effective volume of this container is controlled by the parameters, κ and b. In our calculations, $\kappa=12$. Three different values of b were used. The system used in the simulations consists of $N=108$ WCA particles interacting with a pairwise Lennard-Jones potential $\psi(r)=4\varepsilon[(\sigma/r)^{12}-(\sigma/r)^6]$, truncated and shifted at its minimum $r/\sigma=2^{1/6}$. The temperature $T_0=0.722$ was used as the target temperature.

In all our work conventional reduced units are used: the length in σ, the energy in ε, and the temperature in ε/k_B; the time unit is $\sigma\sqrt{m/\varepsilon}$. The Q parameter is in the Lennard-Jones units ε. The equations of motion were solved using the classic fourth-order Runge-Kutta method, with a time step of $\Delta t=0.001$.

First, the NH dynamics has been used to equilibrate the system at given conditions, (κ,b,Q,T_0,N). Next, starting from the well equilibrated state, long runs have been performed with the NH and GNH dynamics. In the case of the NH dynamics usually less then 2×10^4 time steps were sufficient to achieve the target temperature. In contrast, even after hundreds of thousands of time steps (more than an order of magnitude longer than usually is needed in MD simulations) the average kinetic temperature produced by the GNH dynamics was still different from T_0. This rather disappointing result is shown in Fig. 1. In the figure deviations of the average kinetic temperature from T_0 are shown for three different effective densities which are determined by the external potential with $b=10^{-4}$, 10^{-5}, and 10^{-6}. The data obtained for different Q's are also demonstrated. The results in Fig. 1 clearly indicate that, in contrast to the correct average temperature produced by the NH dynamics, the GNH dynamics produces an average ''temperature'' which changes continuously in time with characteristic oscillations depending upon the system and dynamics parameters.

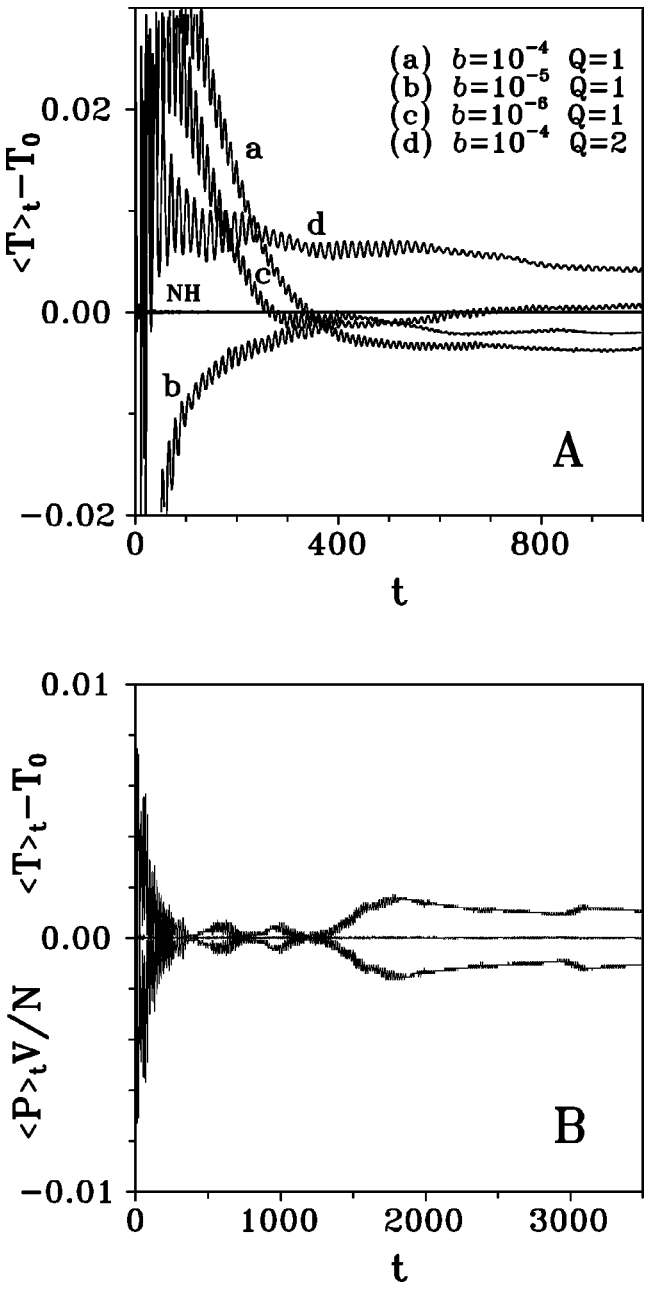

FIG. 1. (A) Deviations of the average kinetic temperature from the target temperature $T_0=0.722$ as a function of accumulated simulation time, t, in the system of $N=108$ WCA particles in external potential (see the description in the text). The four curves (a)–(d) were obtained at different system and dynamics conditions (b,Q) under the GNH dynamics in which the particle position scaling was exploited [Eqs. (22)–(25)]. The corresponding four curves obtained under the NH dynamics are indistinguishable, and on the scale of the graph are seen as a zero deviation on a straight line. (B) Example of a realization of the condition $2(\langle K\rangle-K_0)=-3V\langle P\rangle$ [see Eq. (26)]. The horizontal line is the sum of the curves. Data are from a continuation of the simulation which produced curve (c) in (A).

Some explanation of this problem can be deduced directly from the form of the GNH equations of motion. As one can note, Eq. (24) has the form

$$Q\frac{d\zeta}{dt}=2(K-K_0)+3VP, \tag{26}$$

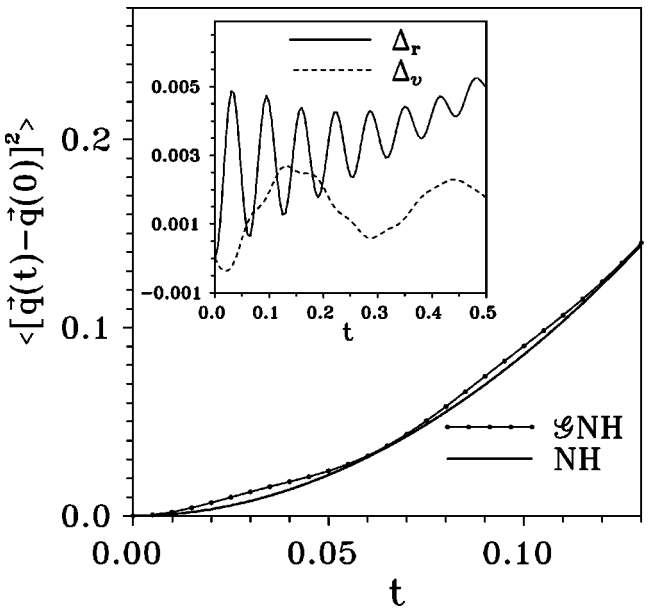

FIG. 2. Mean square displacement in the system of WCA particles in the external potential ($N=108$, $T_0=0.722$, $Q=1$, $b=10^{-6}$) calculated with the NH and GNH dynamics (22)–(25). The inset shows a difference (Δ_r) between the mean square displacements obtained with these dynamics (solid line). Dashed line shows the corresponding difference (Δ_v) between the velocity autocorrelation functions.

where K denotes instantaneous kinetic energy, K_0 represents the average kinetic energy (corresponding to the given temperature, T_0), and V is a volume. As we consider a system in an external potential, P represents here instantaneous difference between the external pressure (due to the external force) and the internal pressure (due to the interparticle forces), and in accordance with the virial theorem its average has to be zero (irrespective of the form of interparticle interactions) [6]. Equation (26) indicates that the dynamics [Eqs. (22)–(25)] does not guarantee that the separate relations $\langle P\rangle=0$ and $\langle K\rangle=K_0$ can be achieved. Instead, it indicates that the more general condition $2(\langle K\rangle-K_0)=-3V\langle P\rangle$ will be realized. With this condition, however, the GNH dynamics can produce different dynamical states which do not necessarily give correct averages of the physical quantities. This problem is illustrated in Figs. 1(B) and 2. Figure 1(B) shows results of a very long run, which was a continuation of the simulation producing the curve (c) in Fig. 1(A). The two curves in the figure, representing $V\langle P\rangle/N$ and deviations of the average kinetic temperature, clearly demonstrate that the desired physical conditions $\langle P\rangle=0$ and $\langle K\rangle=K_0$ can never be achieved in the system. Figure 2 shows the difference between the autocorrelation functions (ACF's) obtained with the GNH and NH dynamics. For short-time periods, considered in the figure, the mean square displacement and the velocity ACF's calculated with the NH method are, as expected, smooth and monotonic functions of time. As the accuracy of the ACF's at short-time periods is very high, the same results should be obtained from the GNH scheme. However, as is clearly visible in Fig. 2, the results are significantly different. The apparent artificial oscillations produced by the GNH dynamics indicate unequivocally that this dynamics is not able to reproduce correctly the system's physical quantities such as the one-particle ACF.

On the basis of the above results we can conclude that the GNH dynamics in the form given by Eqs. (22)–(25) cannot guarantee that the target temperature will be achieved in a system of interacting particles in the external field. Furthermore, some unphysical (oscillatory) behavior of calculated quantities can occur. Let us note that the above considerations and conclusions also remain valid for the whole class of GNH dynamics defined by the $h=sf$, $w=s$, and $f=s^l$ functions.

Next we considered an infinite periodic system used in the computer simulations. First we applied the NH equations to a system of 108 WCA particles in periodic boundary conditions in the solid state (an initial configuration was the face-centered-cubic lattice, and V was a cube). Simulations were performed at several different state (T_0,V) conditions. Usually fewer than 5×10^4 time steps were sufficient to establish the desired temperature, and obtain correct values of physical quantities such as the energy or pressure.

Application of Eqs. (22)–(25) to the well equilibrated WCA solid, at any of the considered state conditions, led quickly to a significant changes in the monitored instantaneous physical quantities, and the desired value of the average kinetic temperature (as well as other physical quantities) was not achieved, even after long-time simulations. The calculations were repeated for a system of 256 Lennard-Jones (LJ) particles. The results were similar to that for the WCA system. In Fig. 3 the evolution of the instantaneous temperature, generated by the NH and GNH equations, in the LJ system is shown at two thermodynamic states ($T_0=0.43$, $N/V=1.00$) and ($T_0=0.63$, $N/V=1.00$). After the reduced time periods of 40, the temperature T_0 was switched from 0.43 to 0.63, or vice versa. An initial state point was from a well equlibrated, with the NH dynamics, fcc solid at $T_0=0.43$ [Figs. 3(a) and 3(b)], and at $T_0=0.63$ [Fig. 3(c)]. It has been checked for $Q\in(0.05,50)$ that the results shown in Fig. 3 are fairly insensitive to a particular value of the Q parameter. It is obvious from the figure that the GNH dynamics produces incorrect and history-dependent results, and $\langle T\rangle\neq T_0$. The pressure and the total potential energy display similar an unphysical behavior, and are strongly correlated with the temperature.

However, the GNH dynamics seems to be established in conceptually consistent steps incorporating the ensemble-ensemble, ensemble-dynamics, and dynamics-dynamics relations. So, what is incorrect? To find the reason for the failure of the GNH approach, let us note that the volume V' in the virtual space cannot (as usually) be fixed because, otherwise, one would obtain the incorrectly established ensemble-ensemble relation. The ensemble-ensemble relation is based on the simple proportionality relation between the microcanonical partition function of the extended virtual system and the canonical partition function of the physical system [Eq. (4)]. To derive this relation one has to change the variables (from primed to unprimed) in accordance with the scaling relations (1) or (12), and integrate over the variable s [12]. However, for a fixed volume in virtual space the scaling of virtual particle positions causes the integration limits of the physical positions to become s dependent, and consequently the integration over the variable s, which is necessary to

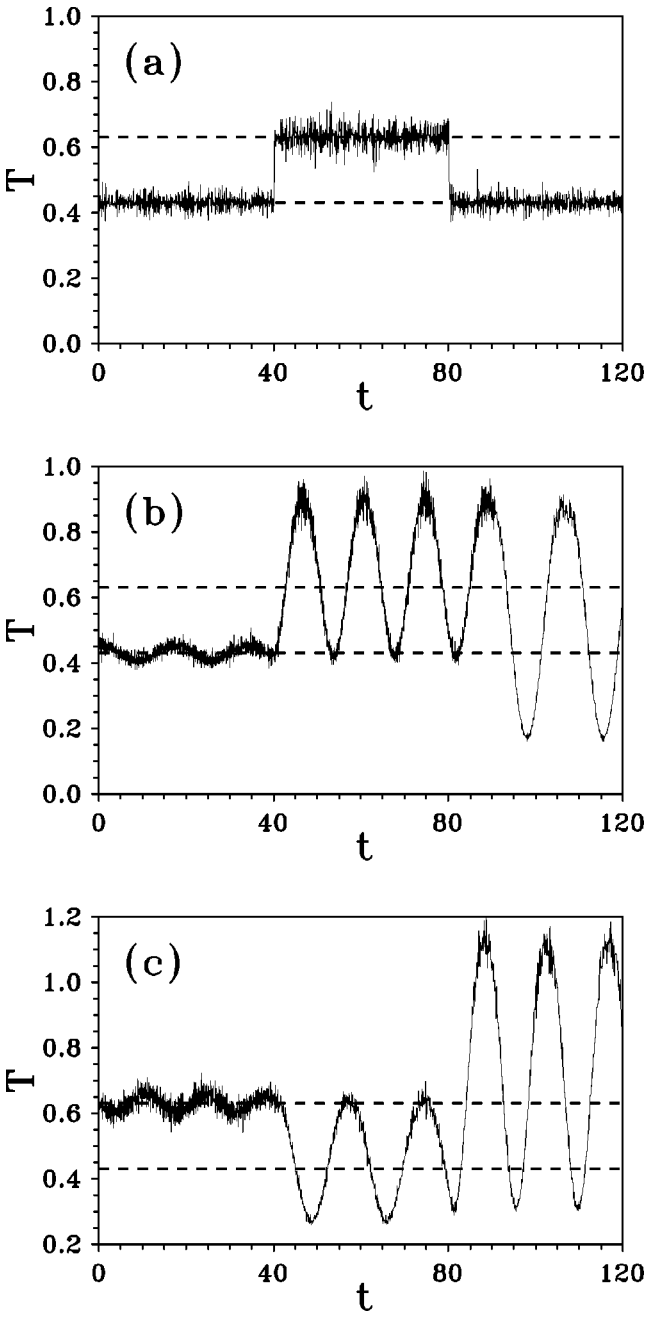

FIG. 3. Evolution of the instantaneous temperature T in the Lennard-Jones system ($N=256$, $N/V=1.00$, $Q=1$) obtained from the NH dynamics (a), and from the GNH dynamics (b) and (c), at two temperatures $T_0=0.43$ and 0.63 (indicated as the dashed lines). An initial state point was from a well equilibrated (with the NH dynamics) fcc solid. At a reduced time $t=40$ the temperature T_0 was changed to 0.63 [to 0.43 in (c)], and at $t=80$ it was switched back to 0.43 [to 0.63 in (c)].

obtain the canonical distribution, cannot be performed prior to the integration over the positions (as far as the scaling functions f_i are not constants).

Hence the only possiblity is to assume that the volume of the virtual system scales with the f function, $V'=V/f^D(s)$, where D is the dimensionality of the system [18]. (In general, if f_i were different, a ''volume'' accessible to each virtual particle would be different and would vary according to changes of the f_i function.) In this case, after performing the position transformation $\mathbf{q}=\mathbf{q}'f(s)$, the integration limits of the physical (unprimed) positions become fixed and the s integration can be formally performed, establishing the desired ensemble-ensemble relation. However, the problem with this interpretation is that, except in the trivial case where $f(s)$ is constant, contrary to the case of any microcanonical ensemble considered in the framework of statistical mechanics, the volume of the system in the virtual space is not fixed but varies as a reaction to the s-variable ''motion.'' Thus the volume of the virtual system is no longer a fixed parameter but becomes a *variable* which has a close parallel to the situation in isothermal-isobaric dynamics [9]. In the isothermal-isobaric dynamics the time dependent volume and its conjugate momentum are explicitly present in the equations of motion for the extended virtual system. In the case considered here, the volume, which is implicitly time dependent through the s variable, is not included in the generalized Hamiltonian or in the derived equations of motion. Consequently it is not a surprise that the dynamics based on the generalized Hamiltonian yields unphysical behavior.

It is worth adding that, from a formal point of view, considering a system with a volume which scales with an s-dependent function, one also encounters a very basic problem of classical mechanics in which the canonical coordinates are not all independent but are connected through equations of nonholonomic constraints. As there is no straightforward approach available to deal with the nonholonomic constraints, usually each case must be tackled individually [23]. Thus, before considering the dynamics-ensemble and dynamics-dynamics relations, one should first determine the appropriate Lagrange equations for the system in the virtual space which takes into account the nonholonomic constraints connected with varying s-dependent volume. Obviously, such equations, if determined, would be in general different from the GNH scheme.

On the basis of the above results and discussion, we conclude that, not only the special case given by Eqs. (22)–(25), but any GNH dynamics which involves position scaling functions, is expected to produce noncanonical averages, and cannot guarantee that the target temperature will be achieved in the system. In accordance with this conclusion, the GNH equations of motion (18)–(21), reduce to the following form:

$$\frac{d\mathbf{q}_i}{dt}=\frac{w}{h_i}\frac{\mathbf{p}_i}{m}, \tag{27}$$

$$\frac{d\mathbf{p}_i}{dt}=-\frac{w}{h_i}\frac{\partial U}{\partial \mathbf{q}_i}-\frac{1}{h_i}\frac{dh_i}{ds}\frac{w}{uQ}P_s\mathbf{p}_i, \tag{28}$$

$$\frac{ds}{dt}=\frac{w}{uQ}P_s, \tag{29}$$

$$\frac{dP_s}{dt}=\frac{w}{u}\left(\sum_i \frac{\mathbf{p}_i^2}{m}\frac{1}{h_i}\frac{dh_i}{ds}-kT\frac{dv}{ds}\right), \tag{30}$$

where we set all the irrelevant constants $f_i\equiv 1$.

V. TIME SCALING

The time scaling, explicitly represented in the GNH equations through the scaling function w, has been considered as a totally independent procedure, not related to the variable transformations between physical and virtual systems [18,15]. Nosé [5] pointed out that this is true only for static quantities. For dynamic quantities he postulated that the force derived from the potential should be identical with that in Newton's equation, and consequently the following relations are required: $wf_i/h_i=1$. In this section we show that this requirement is a sufficient condition but not a necessary one, and demonstrate, based on statistical mechanical arguments, why the time scaling is not an independent transformation.

Let us first briefly discuss the static quantities. To find and exploit any potential advantages of the time scaling extra flexibility of the GNH equations of motion, we performed MD simulations of the WCA fluid with periodic boundary conditions at the state points $T_0=0.722$, and $\varrho=0.8442$ (which corresponds, roughly to the triple point of the Lennard-Jones liquid). The chosen system is an inherently mixing system and is often used as a reference state for testing MD procedures.

In the simulations presented in this section the following form of the scaling functions was chosen : $w(s)=s^l$, $u(s)=1$, $h_i(s)=s$, and $v(s)=g\ln s$, where l is a real number, $g=n+1-l$, and n is a number of the degrees of freedom of the physical system. With these scaling functions the GNH equations of motions are equivalent to those discussed by Jellinek (see Eqs. (40) in Ref. [18]) and read

$$\frac{d\mathbf{q}_i}{dt}=\frac{s^l}{s}\frac{\mathbf{p}_i}{m}, \tag{31}$$

$$\frac{d\mathbf{p}_i}{dt}=-\frac{s^l}{s}\left(\frac{\partial U}{\partial \mathbf{q}_i}-\frac{1}{Q}P_s\mathbf{p}_i\right), \tag{32}$$

$$\frac{ds}{dt}=\frac{1}{Q}s^lP_s, \tag{33}$$

$$\frac{dP_s}{dt}=\frac{s^l}{s}\left(\sum_i\frac{\mathbf{p}_i^2}{m}-kTg\right). \tag{34}$$

The WCA fluid used in the simulations consisted of $N=108$ particles, and the simulations were carried out for half a million time steps. In the calculations $Q=0.5$ was used as an optimal Q-parameter value (this value was established in preliminary simulations with the NH thermostat).

Calculations performed with different l gave correct average kinetic temperature equal to the target temperature T_0. As one can see in Table I, other static quantities, like the total energy and pressure, also depend very little on the particular value of l. Thus, in accordance with the theoretical predictions, the GNH equations of motion with different time scaling functions produce the same averages of static quantities. However, the various alternative dynamical procedures, defined by different l, differ considerably in the convergence rates of calculated quantities. The convergence of static quantities to their correct final values becomes increasingly sluggish as l deviates from unity. In all the studied cases the fastest convergence was achieved with the NH dynamics ($l=1$). Thus the extra flexibility coming from the time scaling does not seem to lead to any practical advantages.

TABLE I. The properties of the WCA fluid calculated under the GNH dynamics with different time scaling functions $w=s^l$ [Eqs. (31)–(34)] ($N=108$, $T_0=0.722$, $\varrho=0.8442$, and $Q=0.5$). The columns from left to right: the time scaling function, average kinetic temperature, total potential energy per particle, pressure, diffusion coefficient from Eq. (35), and diffusion coefficient from Eq. (36). The last two rows represent the data obtained under the specially prepared GNH dynamics in which $\langle s^{l-1}\rangle$ was close to unity.

l	$\langle T\rangle$	$\langle U\rangle$	$\langle P\rangle$	Dv	Dr
1	0.7220	0.716(3)	6.328(5)	0.039	0.039
2	0.7220(1)	0.717(3)	6.330(6)	0.046	0.035
4	0.7220(2)	0.716(5)	6.325(7)	0.061	0.027
6	0.722(1)	0.714(8)	6.32(1)	0.083	0.021
6	0.7220(5)	0.716(6)	6.327(6)	0.039	0.040
2	0.7220(1)	0.717(3)	6.330(6)	0.039	0.039

Let us now consider results for dynamic quantities. Figure 4(a) clearly shows that the velocity autocorrelation function $C_v(t)=\langle\mathbf{p}(t)\mathbf{p}(0)\rangle/3$, depends strongly on the particular form of the time scaling function. Also the mean square displacement [Fig. 4(b)] depends significantly on l. In the last two columns in Table I, the self-diffusion coefficients calculated from the Green-Kubo relation,

$$D_v=\int_0^\infty C_v(t)dt, \tag{35}$$

and from the mean square displacement, at $t\to\infty$,

$$D_r=\frac{1}{6t}\langle(\mathbf{q}(t)-\mathbf{q}(0))^2\rangle, \tag{36}$$

are shown. Within the statistical uncertainties, both of the autocorrelation functions must produce the same diffusion coefficient $D_v=D_r$. As one can see comparing the first row with the last two rows in Table I, the consistent results can be obtained not only for $l=1$ but also with the dynamics defined by $l\neq1$.

An explanation of this problem can be obtained by following the method by Evans and Holian [20] to show the thermodynamic equivalence of the NH and Newtonian equilibrium time correlation functions. Using their approach, let $C(t_N)$, $C(t_{GNH})$ denote equilibrium time correlation functions of the extensive phase variables A and B with zero mean computed under Newtonian and GNH dynamics, respectively. The difference between them, ΔC, can be estimated considering the difference, ΔL, between the Newtonian and GNH Liouvilleans [20]

$$\Delta L=\left(\frac{s^l}{s}-1\right)\sum_i\mathbf{p}_i\frac{\partial}{\partial\mathbf{q}_i}+\left(\frac{s^l}{s}-1\right)\sum_i\mathbf{F}_i\frac{\partial}{\partial\mathbf{p}_i}$$
$$-\zeta\frac{s^l}{s}\sum_i\mathbf{p}_i\frac{\partial}{\partial\mathbf{p}_i}+\dot\zeta\frac{\partial}{\partial\zeta}+\dot s\frac{\partial}{\partial s}, \tag{37}$$

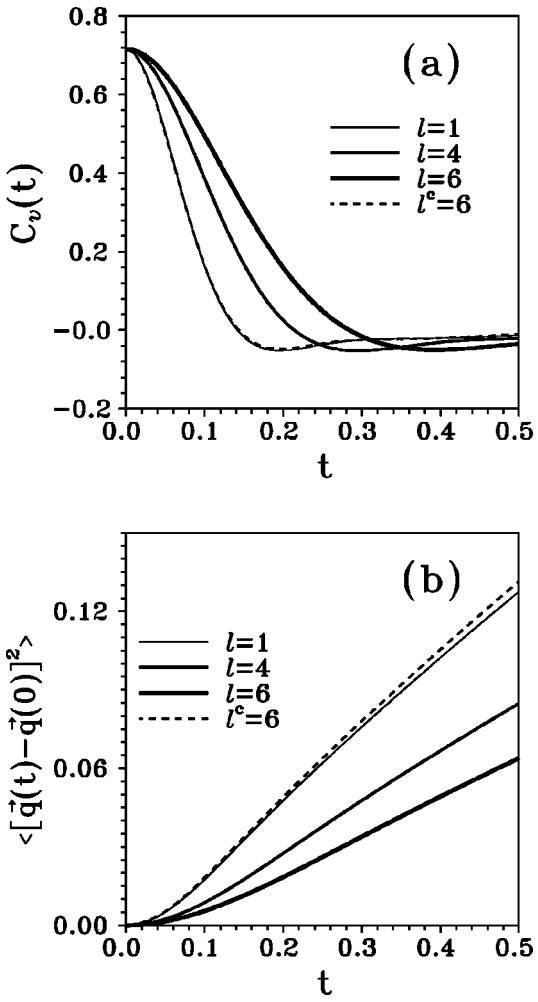

FIG. 4. Velocity autocorrelation functions (a), and mean square displacements (b), of the WCA fluid obtained under the GNH dynamics [Eqs. (31)–(34)], with different time scaling functions $w=s^l$ ($l=1$ corresponds to the NH dynamics; for $l>1$, the average of s^{l-1} was greater than 1.2). Dashed curves represent the data obtained under the specially prepared GNH dynamicas, labeled by l^c, in which the resulting time average of s^{l-1} was very close to unity ($\langle s^{l-1}\rangle \approx 1.03$, $l=6$).

where $\mathbf{F}_i=-\partial U/\partial \mathbf{q}_i$, and $\zeta=P_s/Q$. The last two terms can be ignored in further considerations, since phase variables of interest will not usually have any explicit dependence upon ζ and s. The first three terms give

$$\Delta C(t)=\int_0^t d\tau\left\langle A(\tau-t)\left(\frac{s^l}{s}-1\right)B'(\tau)\right\rangle + \int_0^t d\tau\left\langle A(\tau-t)\left(\frac{s^l}{s}-1\right)B''(\tau)\right\rangle - \int_0^t d\tau\left\langle A(\tau-t)\zeta\frac{s^l}{s}B'''(\tau)\right\rangle, \tag{38}$$

where B', B'', and B''' are new extensive variables resulting from transformation of the variable B under the operators $\Sigma_i \mathbf{p}_i\partial/\partial\mathbf{q}_i$, $\Sigma_i \mathbf{F}_i\partial/\partial\mathbf{p}_i$, and $\Sigma_i \mathbf{p}_i\partial/\partial\mathbf{p}_i$, respectively. As $\langle\zeta s^{l-1}\rangle=0$ and ζs^{l-1} is intensive, the last integral is of order $1/N$ of $C(t_N)$ [20]. Also $s^l/s-1$ is an intensive variable but the first two integrals will be of order $1/N$ of $C(t_N)$ only if the condition $\langle s^{l-1}\rangle=1$ is obeyed. This is just the condition which must be satisfied if dynamic quantities are to be correctly determined (see the data in the last two rows in Table I). Obviously this condition is exactly obeyed if $l=1$. For $l\neq 1$, incorporating the constraint $\langle s^{l-1}\rangle=1$ into the equations of motion is rather a hopeless task. Thus, use of any GNH dynamics with $l\neq 1$ would in practice usually require, at any state point, a long additional preliminary numerical search for the appropriate condition (i.e., an initial point in $\{\mathbf{q},\mathbf{p},s,\zeta\}$), which gives $\langle s^{l-1}\rangle\cong 1$. (For larger systems of at least a few hundred particles, the constraint can be well approximated by the more manageable condition $\langle s\rangle=1$). Furthermore, in any practical realization the condition can be obeyed only with some finite accuracy, which means that calculated dynamical quantities will inevitably be only approximate, and therefore unreliable to some extent (see the data represented by the dashed line in Fig. 4). In this sense any practical realization with $l\neq 1$ is incorrect.

The above reasoning can be extended to any time and momentum scaling functions and, hence, we come to the important conclusion that the time scaling is *not* an independent procedure. The time scaling function w must obey the conditions $\langle w/h_i\rangle=1$. Although these conditions are sufficient for calculations of the equilibrium time correlation functions, the difficulty in incorporating them into the equations of motion means that in practice *only* the choice $w\equiv h_i$ can be considered, which is consistent with Nosé's requirement.

An important consequence of the latter condition is that all h_i functions have to be the same. Thus, the GNH equations of motion (27)–(30) further reduce their generality to the following form:

$$\frac{d\mathbf{q}_i}{dt}=\frac{\mathbf{p}_i}{m}, \tag{39}$$

$$\frac{d\mathbf{p}_i}{dt}=-\frac{\partial U}{\partial \mathbf{q}_i}-\frac{1}{u}\frac{dh}{ds}\frac{P_s}{Q}\mathbf{p}_i, \tag{40}$$

$$\frac{ds}{dt}=\frac{h}{u}\frac{P_s}{Q}, \tag{41}$$

$$\frac{dP_s}{dt}=\frac{h}{u}\left(\frac{1}{h}\frac{dh}{ds}\sum_i\frac{\mathbf{p}_i^2}{m}-kT\frac{dv}{ds}\right). \tag{42}$$

The above equations, comprising three functions h,v, and u and a single parameter Q, are the most general form of the GNH equations of motion that are able to generate correctly both static and dynamic properties of a system at equilibrium.

VI. SCALING OF VIRTUAL MOMENTUM

Scaling of the P_s' variable has also been considered as an additional transformation generating canonical dynamics in physical space [15,24,18]. It can be shown, however, that this transformation always leads to the same form of equations of motion. Instead of the transformation $P_s=P_s'/u$ let us consider the more general relation $P_s=P_s'/\mathcal{V}$, where $\mathcal{V}$ is

some real differentiable function of s (in general different from u). With this relation the GNH equations are

$$\frac{d\mathbf{q}_i}{dt}=\frac{\mathbf{p}_i}{m}, \tag{43}$$

$$\frac{d\mathbf{p}_i}{dt}=-\frac{\partial U}{\partial \mathbf{q}_i}-\frac{1}{u}\frac{dh}{ds}\frac{\mathcal{V}}{u}\frac{P_s}{Q}\mathbf{p}_i, \tag{44}$$

$$\frac{ds}{dt}=\frac{h}{u}\frac{\mathcal{V}}{u}\frac{P_s}{Q}, \tag{45}$$

$$\frac{dP_s}{dt}=\frac{h}{u}\frac{u}{\mathcal{V}}\left(\frac{1}{h}\frac{dh}{ds}\sum_i\frac{\mathbf{p}_i^2}{m}-kT\frac{dv}{ds}\right)+\left(\frac{\dot{u}}{u}-\frac{\dot{\mathcal{V}}}{\mathcal{V}}\right)P_s, \tag{46}$$

where

$$\dot{u}=\frac{du}{ds}\frac{h\mathcal{V}}{u^2}\frac{P_s}{Q}, \qquad \dot{\mathrm{V}}=\frac{d\mathcal{V}}{ds}\frac{h\mathcal{V}}{u^2}\frac{P_s}{Q}.$$

With the new variable $P_s^*=\mathcal{V}P_s/u$, the above equations become independent of $\mathcal{V}$ and are exactly the same as the GNH equations (39)–(42).

VII. EQUILIBRIUM PROPERTIES OF GNH DYNAMICS

Any practical realization of the GNH equations requires specification of three functions h,u, and v. It is worth stressing that these functions are not arbitrary real differentiable functions of s. The ensemble-ensemble relation, discussed above in Sec. II, requires, e.g., that the following condition must be obeyed by these functions [12]:

$$\frac{u(v^{-1})}{v'(v^{-1})}h^{3N}(v^{-1})\sim\exp(-H(\mathbf{p},\mathbf{q})/kT), \tag{47}$$

where v', and v^{-1} denote dv/ds and the function inverse to v, respectively (the functions are taken at a single solution s_0 of the equation $H'_{G\mathcal{N}}-E=0$). The above condition considerably limits the number of possible forms of the h,u, and v functions. For example, a logarithmic form of the v function implies a power form of the h function, and, vice versa a power h function implies a logarithmic v function. If v is to be a linear function of s, then the h function has to be an exponential, and if h is to be an exponential then v has to be a linear function.

In searching for possible advantages of the GNH dynamics we limit our further considerations to only one set of functions obeying condition (47). That is, we consider the case $v=g\ln s$, $h=s^\alpha$, and $u=s^\vartheta$, which seems to be the most reasonable and promising for practical applications. α,ϑ are real numbers and $g=(n-1)\alpha+1+\vartheta$. For $\alpha=1$ and $\vartheta=0$ the equations are the NH equations, and the case $\alpha=2$, $\vartheta=0$ was considered by Winkler [15].

A valuable feature of this set of functions is that the resulting GNH equations can be converted to the form

$$\frac{d\mathbf{q}_i}{dt}=\frac{\mathbf{p}_i}{m}, \tag{48}$$

$$\frac{d\mathbf{p}_i}{dt}=-\frac{\partial U}{\partial \mathbf{q}_i}-\zeta\mathbf{p}_i, \tag{49}$$

$$\frac{d\sigma}{dt}=\zeta, \tag{50}$$

$$\frac{d\zeta}{dt}=\frac{1}{Q}\left(\sum_i\frac{\mathbf{p}_i^2}{m}-gkT\right)e^{2\epsilon\sigma}+\epsilon\zeta^2, \tag{51}$$

where now $g=n-\epsilon$. To derive these equations of motion from the GNH equations (39)–(42) the following substitutions have been made: $\sigma=\alpha\ln s$, $\zeta=\alpha Q^{-1}P_s s^{\alpha-\vartheta-1}$, and $\epsilon=(\alpha-\vartheta-1)/\alpha$, and the Q parameter has been replaced by Q/α. In the following we will denote Eqs. (48)–(51) as extended NH (ENH) equations. The ENH equations can be shown to have the phase-space distribution

$$\mathcal{F}_c\propto\exp\left(-\frac{1}{kT}\left[\sum_i\frac{\mathbf{p}_i^2}{2m}+U(\mathbf{q})+\frac{1}{2}Q\zeta^2e^{-2\epsilon\sigma}+kT\sigma\right]\right), \tag{52}$$

and the conserved quantity of this system is

$$\Upsilon=\sum_i\frac{\mathbf{p}_i^2}{2m}+U(\mathbf{q})+\frac{1}{2}Q\zeta^2e^{-2\epsilon\sigma}+gkT\sigma. \tag{53}$$

The ENH scheme depends only on two parameters (i.e., Q, and ϵ) and is very similar to the NH approach ($\epsilon=0$). In particular, it possesses the frictional force term of the form $-\zeta\mathbf{p}$ common to all deterministic computationally useful approaches to thermomechanics [8]. [Note that the GNH equations (39)–(42) can also be converted to the form with the friction force term $-\zeta\mathbf{p}$ but at the expense of a more complex form for the thermostatting part of the equations.] It can be also readily implemented in an existing MD code.

A special case, $\epsilon=0.5$, has been considered by Winkler *et al.* [23] (note that in our notation $\sigma=2\eta$ and $\zeta=2p_\eta/Q$), and recommended as more nonlinear than the NH equations. The authors argued that their extension was able to produce trajectories that were sufficiently chaotic to calculate average properties of canonical ensemble, even for a small number of degrees of freedom, such as a one-dimensional harmonic oscillator or a single particle confined in the double-well potential.

It is natural to expect that the ENH equations can produce even more chaotic behavior if an optimal value of the parameter ϵ is applied. It is readily shown, for instance, that in the case of a harmonic oscillator, the ENH thermostat produces fairly chaotic trajectories for a range of ϵ and Q values for which the position and momentum distribution functions are close to the exact values. Also, changes in the initial conditions have no appreciable effect on the results. Examination of the first few moments of the position and momentum distribution functions showed that the best performance has been achieved for $0.1<\epsilon<0.4$ and $0.001<Q<0.1$, and an example is shown in Fig. 5.

The apparent ability of the ENH equations to thermalize even such ''pathological'' systems as a one-dimensional harmonic oscillator allows us to consider the ENH thermostat as an effective and alternative method to other thermostatting

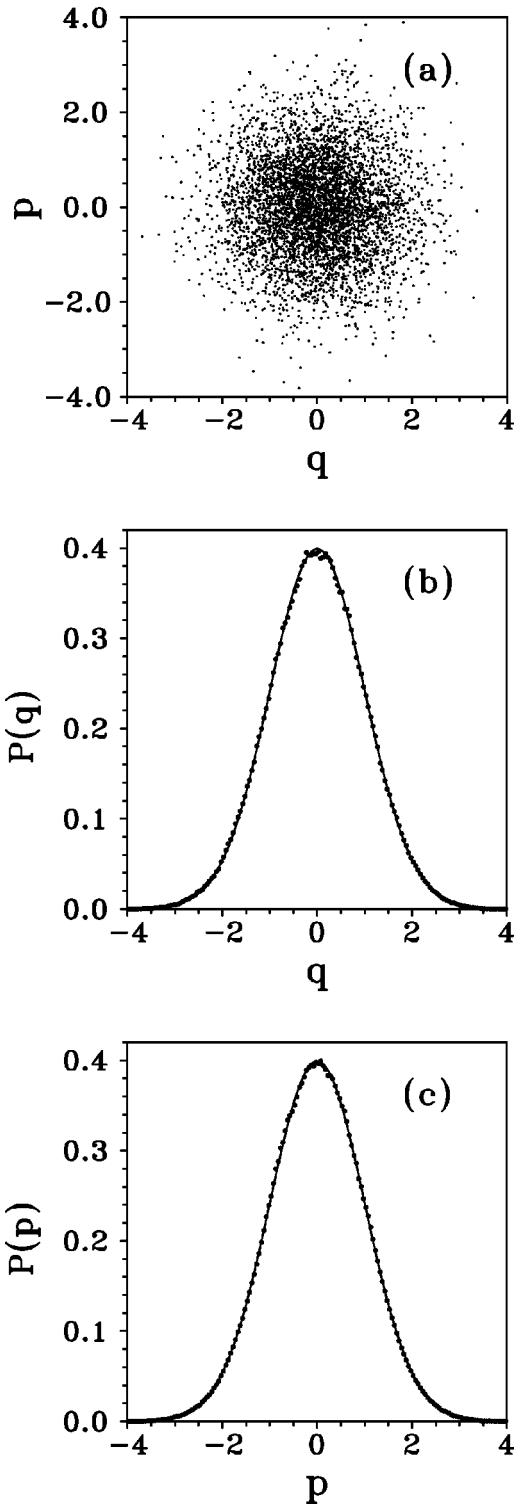

FIG. 5. (a) Density plot of a harmonic oscillator ($m=1$, $\omega=1$, $kT=1$) obtained under the ENH dynamics ($\epsilon=0.2$, $Q=0.01$). (b) and (c) show (dots) the corresponding position and momentum distribution functions, respectively. The data were obtained from simulations made up of 5×10^7 fourth-order Runge-Kutta time steps of length 0.001. The initial condition were $\{q,p,\sigma,\zeta\}=\{1,1,0,1\}$. The solid lines in (b) and (c) are the exact results.

schemes [14,13,16,17] which have been proposed to deal with small or stiff systems, for which the NH and Gaussian thermostats fail. We also stress that, among these schemes, the ENH method is the only one which is Hamiltonian based. Furthermore, if the constant of motion is to be monitored (which is a rather common procedure in MD simulations), the ENH approach will require the least number of thermostatting equations (i.e., two).

We add that in the above WCA-fluid case, at the Lennard-Jones triple point state, which is a system with good mixing, we noted only a marginal improvement over the NH dynamics in the convergence rate of the calculated quantities if the ENH dynamics were used with $0.1<\epsilon<0.3$.

VIII. NONEQUILIBRIUM PROPERTIES OF GNH DYNAMICS

Among the desirable properties of any thermostat the important property is its applicability away from equilibrium. In order to test the applicability of the GNH dynamics away from equilibrium, we considered a WCA fluid subject to a Couette shear strain rate field. The equations of motion were the following thermostatting Sllod (so-named because of its close relationship to the Dolls tensor algorithm) equations [7]

$$\frac{d\mathbf{q}_i}{dt}=\frac{\mathbf{p}_i}{m}+\mathbf{x}\gamma y_i, \tag{54}$$

$$\frac{d\mathbf{p}_i}{dt}=-\frac{\partial U}{\partial \mathbf{q}_i}-\mathbf{x}\gamma p_i,-\zeta\mathbf{p}_i. \tag{55}$$

In these equations $\mathbf{p}_i$ are the peculiar momenta of particle i, $\mathbf{x}$ is the unit vector in the x direction, and γ is the imposed strain rate. The thermostatting mechanism, represented by ζ, was driven by the ENH thermostat [Eqs. (50) and (51)]. The state point simulated were, as previously, $T_0=0.722$ and $\varrho=0.8442$. The simulated WCA fluid consisted of $N=108$ particles, and calculations were performed at the reduced shear rate $\gamma=1$. Calculations performed with different values of the parameter ϵ revealed that direct application of the ENH thermostat with $\epsilon\neq0$ causes similar problems to those observed recently in the case of the Nosé-Hoover chain (NHC) thermostats [25,26]. Thus, we have to conclude that the ENH thermostat, in the above form, is not able to give dynamics consistent with the desired target temperature for a system out of equilibrium.

This unacceptable feature of the ENH thermostat is also expected for other forms of the GNH equations (i.e., for other sets of h, v, and u functions). Taking into account the results of this section and previous sections, one may conclude that the generalization of Nosé Hamiltonian (12), which provides the Hamiltonian basis for the GNH dynamics reduces in practical realizations to the original Nosé Hamiltonian and the NH scheme.

We also note that in parallel to NHC thermostats, a simple modification of the ENH thermostat [Eqs. (50) and (51)], can be proposed (see below), which enables both steady-state averages and time correlation functions to be obtained correctly for nonequilibrium states.

Following the reasoning and results obtained for the modified NHC dynamics [26], we consider the following modified ENH thermostat:

$$\frac{d\zeta}{dt}=\frac{1}{Q}\left(\sum_i \frac{\mathbf{p}_i^2}{m}-gkT\right)e^{2\epsilon\sigma}+\epsilon(\zeta-B)^2, \tag{56}$$

$$\frac{d\sigma}{dt}=\zeta-B. \tag{57}$$

This differs from the original ENH thermostat only in the appearance of a constant B. Repeating our calculations with this modified ENH thermostat, we verified that, as long as B was close to $\langle\zeta\rangle$ and $0.1<\epsilon<0.3$, the SLLOD equations produced results totally consistent with those computed with the Gaussian and NH thermostats [27,26]. (Note that, in equilibrium, $\langle\zeta\rangle=0$, so that the modified ENH equations reduce to the ENH equations). Thus the modified ENH approach can be considered as an extension of the NH scheme. Just as at equilibrium it can offer some advantages in investigations of small or stiff nonequilibrium systems.

IX. CONCLUSIONS

In this work we have demonstrated that any freedom of choice in the selection of the isothermal dynamics schemes based on the generalized Nosé Hamiltonian is largely illusory. We show that the scaling of particle positions with f functions is trivial. All position scaling functions have to be a single constant if canonical averages are to be produced.

If only static quantities are of interest, then time scaling can be considered as an additional procedure to define different generalized Nosé-Hoover dynamics. However, no advantage of using such dynamics for calculating static properties has been found. In all studied cases, the dynamics with different time scaling functions displayed worse convergence rate of calculated quantities than the NH dynamics.

Calculations of equilibrium time correlation functions showed that the time scaling is *not* an independent procedure. Calculations of dynamic quantities require that the average of the ratio of time and momentum scaling functions has to be equal to unity, $\langle w/h\rangle=1$. In practical realizations only the exactly obeyed constraint, i.e., $w\equiv h$ should to be used.

The most general form of the GNH equations has been established, given in Eqs. (39)–(42), which enables the correct calculation of both static and dynamic quantities of a system at equilibrium. It has also been shown that the additional scaling of the momentum of the virtual variable (occasionally exploited to derive different forms of extended dynamics) is irrelevant and leads to the equations of motion which can always be converted to the GNH equations. Thus, the entire generalization of the NH dynamics is, in fact, reduced to *only* two momentum scaling functions h and u, and to a form of the s-variable ''potential energy'' function v.

The remaining three functions h,u, and v involved in the GNH dynamics still offer considerable freedom in selecting the most appropriate and efficient canonical dynamics for a given physical system. These functions are, however, not independent, and only sets of functions obeying the ensemble-ensemble condition (47) need to be considered. The number of such distinct sets which are computationally useful is expected to be very small. The set consisting of logarithmic and power functions was studied in detail as a most promising generalization of the NH dynamics for MD simulations. With this choice of function the GNH scheme becomes very similar to the NH approach but with coupled and more nonlinear thermostatting parts of the equations. These ENH equations (48)–(51) are expected to produce more chaotic phase-space dynamics than the NH equations. We have demonstrated that the ENH dynamics exhibits canonical distribution for a one-dimensional harmonic oscillator. To our knowledge this is the only Hamiltonian based dynamics which possesses such a property.

Direct application of the GNH thermostat to study nonequilibrium problems can be problematic, and in general will lead to incorrect results. In this context the entire generalization reduces to the original NH approach, which can be considered as a fairly unique scheme. However, it has been also demonstrated that, as for the NHC thermostats, a simple modification of the ENH equations is possible, which makes the GNH approach also applicable away from equilibrium.

ACKNOWLEDGMENTS

This work was supported by the Polish Committee for Scientific Research (KBN) Grant No. 8T11F01214. We would like to thank Professor W.G. Hoover for reading the manuscript, and for helpful comments. We thank Professor D. M. Heyes for useful remarks and suggestions. Part of the calculations were performed at the Poznań Computer and Networking Center.

[1] W.G. Hoover and W.T. Ashurst, in *Theoretical Chemistry: Advances and Perspectives*, edited by H. Eyring and D. Henderson (Academic Press, New York, 1975).
[2] H.C. Andersen, J. Chem. Phys. **72**, 2384 (1980).
[3] W.G. Hoover, A.J.C. Ladd, and B. Moran, Phys. Rev. Lett. **48**, 1818 (1982).
[4] D.J. Evans, J. Chem. Phys. **78**, 3297 (1983).
[5] S. Nosé, Prog. Theor. Phys. Suppl. **103**, 1 (1991).
[6] M.P. Allen and D.J. Tildesley, *Computer Simulation of Liquids* (Clarendon Press, Oxford, 1987).
[7] D.J. Evans and G.P. Morris, *Statistical Mechanics of Nonequilibrium Liquids* (Academic Press, London, 1990).
[8] Wm. G. Hoover, *Time Reversibility, Computer Simulation, and Chaos* (World Scientific, Singapore, 1999).
[9] S. Nosé, Mol. Phys. **52**, 255 (1984).
[10] S. Nosé, J. Chem. Phys. **81**, 511 (1984).
[11] W.G. Hoover, Phys. Rev. A **31**, 1695 (1985).
[12] J. Jellinek and R.S. Berry, Phys. Rev. A **38**, 3069 (1988).
[13] A. Bulgac and D. Kusnezov, Phys. Rev. A **42**, 5045 (1990).
[14] I.P. Hamilton, Phys. Rev. A **42**, 7467 (1990).
[15] R.G. Winkler, Phys. Rev. A **45**, 2250 (1992).
[16] G.J. Martyna, M.L. Klein, and E. Tuckerman, J. Chem. Phys. **97**, 2635 (1992).
[17] W.G. Hoover and B.L. Holian, Phys. Lett. A **211**, 253 (1996).
[18] J. Jellinek and R.S. Berry, Phys. Rev. A **40**, 2816 (1989).
[19] J. Jellinek, J. Phys. Chem. **92**, 3163 (1988).

[20] See, e.g., M. Toda, R. Kubo, and N. Saitô, *Statistical Physics I, Equilibrium Statistical Mechanics* (Springer-Verlag, Berlin, 1983).
[21] D.J. Evans and B.L. Holian, J. Chem. Phys. **83**, 4069 (1985).
[22] C.P. Dettmann and G.P. Morriss, Phys. Rev. E **55**, 3693 (1997).
[23] H. Goldstein, *Classical Mechanics*, 2nd ed. (Addison-Wesley, Reading, MA, 1981).
[24] R.G. Winkler, V. Kraus, and P. Reineker, J. Chem. Phys. **102**, 9018 (1995).
[25] B.L. Holian, A.F. Voter, and R. Ravelo, Phys. Rev. E **52**, 2338 (1995).
[26] A.C. Brańka, Phys. Rev. E **61**, 4769 (2000).
[27] D.J. Evans and S. Sarman, Phys. Rev. E **48**, 65 (1993).